




## Article

# A Generalized Automated Framework for Urban Runoff Modeling and Its Application at a Citywide Landscape

Hossein Hosseiny <sup>1,\*</sup> , Michael Crimmins <sup>1</sup>, Virginia B. Smith <sup>1</sup>  and Peleg Kremer <sup>2</sup> <sup>1</sup> Department of Civil and Environmental Engineering, Villanova University, Villanova, PA 19085, USA; mcrimmi2@villanova.edu (M.C.); Virginia.smith@villanova.edu (V.B.S.)<sup>2</sup> Department of Geography & the Environment, Villanova University, Villanova, PA 19085, USA; peleg.kremer@villanova.edu

\* Correspondence: shossein@villanova.edu

Received: 1 January 2020; Accepted: 22 January 2020; Published: 28 January 2020



**Abstract:** This research presents a fully automated framework for runoff estimation, applied to Philadelphia, Pennsylvania, a major urban area. Trends in global urbanization are exacerbating stormwater runoff, making it an increasingly critical challenge in urban areas. Understanding the fine-scale spatial distribution of local flooding is difficult due to the complexity of the urban landscape and lack of measured data, but it is critical for urban management and development. A one-meter resolution Digital Elevation Model (DEM) was used in conjunction with a model developed by using ArcGIS Pro software to create urban micro-subbasins. The DEM was manipulated to account for roof drainage and stormwater infrastructure, such as inlets. The generated micro-subbasins paired with 24-h storm data with a 10-year return period taken from the National Resources Conservation Service (NRCS) for the Philadelphia area was used to estimate runoff. One-meter land-cover and land-use data were used to estimate pervious and impervious areas and the runoff coefficients for each subbasin. Peak runoff discharge and runoff depth for each subbasin were then estimated by the rational and modified rational methods and the NRCS method. The inundation depths from the NRCS method and the modified rational method models were compared and used to generate percent agreement, maximum, and average of inundation maps of Philadelphia. The outcome of this research provides a clear picture of the spatial likelihood of experiencing negative effects of excessive precipitation, useful for stormwater management agencies, city managers, and citizen.

**Keywords:** urban runoff; subbasin delineation; runoff analysis maps

## 1. Introduction

Urban development directly impacts the hydraulic function of watersheds due to changes in land cover and land use and is characterized by increases in impervious areas. Such changes are reflected in alterations to hydrological parameters in watersheds including inundation depth, runoff volume, and the peak discharge of runoff, since impervious areas are the main contributors to surface runoff in urban areas [1,2]. Specifically, increases in impervious areas reduce water travel time through the watershed, thus changing the hydrograph of the watershed, increasing the volume and peak runoff [3] linearly and exponentially, respectively [4].

Urban areas are growing globally, and it is now estimated that 70% of the world's population will reside in urban areas by 2050 [5]. Alteration of hydrographs due to urban growth makes urban areas increasingly susceptible to disruption of key city features and may adversely impact the economy, as well as the health of the environment [6,7].

Estimation of precipitation runoff in urban areas is a major challenge and critically important to city planners, as it affects the daily life of many residents directly and indirectly [8]. For instance, heavy precipitation and high runoff adversely impact traffic flow and the sustainability of city infrastructure.

Quantification of storm runoff is a key factor in the assessment of many environmental processes, such as sediment and pollution transport, and erosion or deposition of the sediment in the watershed [9–12]. Measuring runoff data at large geographic scales is expensive and challenging. As a result, availability of large-scale runoff data is limited. Hence, there is growing interest in developing surface runoff models for current and future scenarios [13,14], allowing for a comprehensive analysis over a large continuous area. Model automation is crucial in such scenarios to allow for processing over large geographic areas by reducing the computation required, potential for error, and work time. Streamlining the processes enables analysis over large continuous spaces, with high-resolution topographic data, previously unattainable.

Subbasins are the preferred hydrological unit for runoff estimation because urban hydraulics is limited by stormwater inlets. Previous studies have shown that spatial processing of high-resolution topographic data is a powerful tool for subbasin delineation [15–17]. Hans et al. [18] demonstrated that identified streams and subbasins are quite sensitive to topographic data resolution. More specifically, low-resolution topographic data do not capture the effects of roads and small drains on flow lines in small watersheds [18,19]. Ji and Qiuwen [16] used modified elevation data to account for the effects of roads, buildings, and conduits on main flow paths in small urban areas. They assumed that the roads and conduits are the main flow path of runoff [16]. The subbasin delineation in these studies are based solely on topographic data, and urban inlets are not considered.

Runoff estimation for large scale watersheds in urban areas is challenging due to the dynamics of parameters affecting surface runoff, including elevation, land cover, and land use. However, simple models for runoff estimation can accurately predict daily event runoff [20,21]. The rational [22] and National Resources Conservation Service (NRCS) methods [3] are two simple, widely accepted, empirically-based models for runoff estimation [23–25]. The rational method was originally developed to assist with the design of sewer and drainage structures by providing an estimated maximum runoff discharge [22,25]. The modified rational method [26] can convert the peak discharge into the volume of runoff by simplifying hydrographs to either a triangular or rectangular runoff hydrograph associated with a design storm [25]. Alternatively, the NRCS method directly estimates runoff depth. The NRCS method is based on the land and soil characteristics of a basin, presented by a curve number (CN). The CN represents the capacity of the soil to absorb generated runoff.

This manuscript presents a fully automated framework to (1) delineate micro-subbasins in a fully urbanized watershed and to (2) estimate the surface runoff for those subbasins by using both the (a) rational and modified rational and (b) NRCS methods. The framework was applied and tested on Philadelphia, a major urban area with frequent flooding issues [27]. In addition, a framework was defined to create runoff base maps for the study area. Such maps aid city managers and residents with identifying critical areas in their local watershed(s), to prioritize required services during flood events. However, the novelty of this work is the integrated methodology and type of data used in this study. The delineated micro-subbasins in the urban environment for each individual stormwater inlet at a citywide scale, coupled with multiple runoff models, result in a unique runoff simulation for the whole city. While such data are scarce, the current framework provides an approach and output required for many other research topics, including social and environmental vulnerability throughout the city to flooding, and green stormwater infrastructure (GSI) effects on runoff reduction.

## 2. Methodology

The primary goal of this research was to estimate runoff in a fully urbanized watershed. Subbasins are the hydrologic units in runoff estimation, and, therefore, the first step is to identify them. This was accomplished through a model developed in Esri's ArcGIS Pro 2.4 software [28], using Arc Hydro extension [29].

The model incorporated high-resolution topography, building footprints, green infrastructure, and stormwater inlets to delineate micro-subbasins for each individual inlet [30,31]. Once subbasins were delineated, the NRCS [32] and modified rational [33] methods were used to estimate surface runoff for each subbasin. To identify areas in the city vulnerable to runoff, runoff depths obtained from both models were integrated and mapped for the whole study area.

### 2.1. Study Area

The study area for this research is the administrative boundaries of Philadelphia, Pennsylvania, a metropolitan city located in the Mid-Atlantic region on the east coast of the US, with a population of more than 1.5 million [34]. The city is highly urbanized, with paved areas accounting for more than 61% of its land cover. Table 1 shows land cover types and the percentage of each class in the study area, based on the one-meter land-cover data [35,36].

**Table 1.** Land types and their coverages within the city of Philadelphia.

Land Type	Area (km <sup>2</sup> )	Coverage (%)
Tree Canopy	74.4	20.2
Grass/Shrub	34.8	9.5
Bare Soil	24.4	6.6
Water	22.5	6.1
Buildings	103.7	28.2
Roads/Railroads	65.0	17.7
Other Paved Surfaces	42.8	11.6

The mean annual precipitation in the city exceeds 1000 mm (40 inches) [37], causing major flooding in the city at least 12 days per year [27,38]. However, the flooding in the city is predicted to increase up to 30–105 days per year by 2050 [27].

In June 2019, a 12 cm precipitation event and flash flood occurred in Philadelphia. As a result, many people were stranded and required assistance from first responders and rescue personnel [39]. As heavy precipitation events in Philadelphia become more prevalent [27] and urban area increases [5], there is expected to be an increase in social demand for flood protection and rescue. This emphasizes the importance of identifying areas vulnerable to flood inundation in urban settings and working toward more efficient stormwater-management strategies for such areas.

The city has a cutting-edge stormwater-management program that promotes research, design, implementation, and maintenance of GSI in urban areas. In addition, there are strict design requirements for stormwater mitigation projects in the city [35]. Nevertheless, urban areas in the city have increased by 11% from 2008 to 2015, while natural areas have decreased by 15%. Philadelphia has a robust and relatively comprehensive online open data platform, which allows access to data necessary for this research. The study area for this research is confined to the city boundary, as shown in Figure 1, due to data availability restrictions.

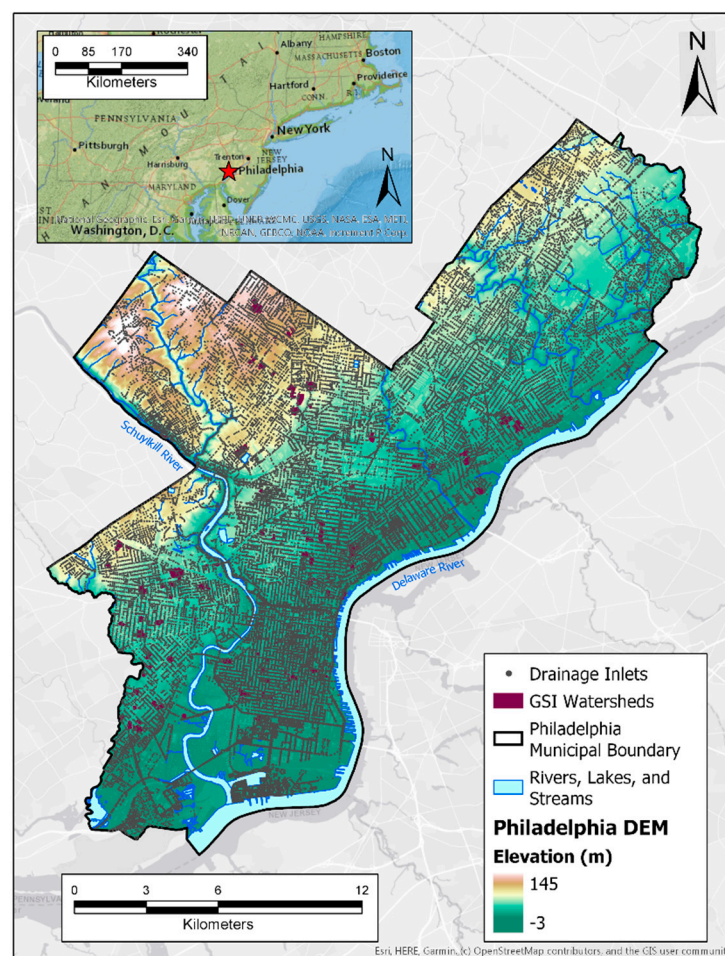


**Figure 1.** The study area of this research is limited to the City of Philadelphia, PA.

## 2.2. Input Data

High-resolution topographic data, preferably one-meter DEM, are required to properly detect flow lines in urban areas [31]. Required data for this study were obtained and integrated from multiple sources, including OpenDataPhilly and the Pennsylvania Spatial Data Access (PASDA) database [40,41]. A summary of the datasets used in this analysis is provided in Table 2.

**Table 2.** Summary of study datasets.

Data	Type	Spatial Resolution (m)	Created by	Source
Digital Elevation Model (DEM) 2015	Raster	1	City of Philadelphia	PASDA [42]
Drainage Inlets	Shape file	-	Philadelphia Water Department	OpenDataPhilly [43]
Municipal Boundary	Shape file	-	Philadelphia Department of Planning and Development	OpenDataPhilly [43]
Hydrologic Features	Shape file	-	Philadelphia Water Department	OpenDataPhilly [43]
Building Footprints	Shape file	-	Philadelphia Department of Licenses and Inspections and Office of Innovation and Technology	OpenDataPhilly [43]
Land cover 2015	Raster	1	Villanova University	[35,36]
Curve Number	Raster	1	Villanova University	[36]
GSI Locations	Shape file	-	Philadelphia Water Department	OpenDataPhilly [43]



### 2.3. Micro-Subbasin Delineation

Previous research has demonstrated proof-of-concept for delineating micro-subbasins by using high-resolution DEMs [30]. However, such studies did not account for drainage inlet location when delineating subbasins [30]. This research builds upon the methodology established in past research but goes one step further by delineating a subbasin for each drainage inlet in Philadelphia. Using ArcPro, the one-meter DEM of Philadelphia was preprocessed in order to create a hydrologically correct DEM. First, the “Fill Sinks” tool was used to smooth the base DEM surface. Drainage inlet and GSI features were buffered by 1 and 0.3 m (3 and 1 feet), respectively. The buffered features and a building footprint feature class were then assigned elevation values and converted to separate raster files. The resulting rasters were then mosaicked with the smoothed base DEM. Inlet and GSI features were sunk into the DEM by 1.5 m (5 feet), while buildings were raised by 9.1 m (30 feet).

Next, the mosaicked DEM was processed by using the “Dendritic Terrain with Unknown Stream Location” workflow in the ArcHydro toolbox. This workflow generates numerous hydrologic outputs, including flow direction and accumulation rasters, stream lines, drainage lines, and drainage catchment polygons. The resulting flow-accumulation raster was used as an input into the “Snap Pour Points” tool, to snap to the highest flow accumulation value within a given distance of each drainage inlet. The selected snapping distance was determined by Equation (1):

$$D = x\sqrt{2}, \quad (1)$$

where  $D$  is the snapping distance, and  $x$  is the cell size of the flow accumulation raster. The  $D$  in Equation (1) is also equivalent to the hypotenuse of a triangle bounded by two adjacent sides of a raster cell. Using this snap distance ensures that each pour point will be snapped to the cell with the highest flow accumulation value within a one-cell radius of each inlet. The “Watershed” tool was used to delineate watersheds for each snapped inlet pour point in a raster file, which was subsequently converted to a polygon feature class. It should be noted that subbasins were delineated based on the identified flow direction within each subbasin and, therefore, did not account for the waterflow between subbasins. The inlet feature class attribute table was then combined with the newly created inlet watershed feature class, using a series of joins. Finally, a building footprint feature class was used to erase all buildings from the inlet watershed polygons. Runoff related to buildings is removed in this analysis because it is assumed that most roof drainage systems in Philadelphia capture runoff from rooftops and route it directly into the stormwater drainage system via roof gutters.

### 2.4. Surface Runoff

Estimating surface runoff at a citywide scale can be carried out via computation within microscale sub-watersheds. This implies the need for use of high-resolution topographic data (less than or equal to one meter) to capture the flow lines within the urban areas.

#### 2.4.1. Design Storm

A standard NRCS 10-year design storm for Philadelphia was selected for this study based on Philadelphia Water Department guidelines [44] for the city inlet and sewer system design. The rainfall distribution of a 24-h storm is presented in Table 3.

**Table 3.** NRCS 10-year, 24-h design storm for Philadelphia, PA.

Duration	10-year Precipitation (mm)	Intensity (mm/h)
5 min	14.7	176.8
10 min	22.9	137.2
15 min	28.2	112.8
30 min	39.6	79.2
1 h	51.6	51.6
2 h	62.5	31.2
3 h	68.8	22.9
6 h	86.4	14.4
12 h	106.7	8.9
<b>24 h</b>	<b>125.7</b>	<b>5.2</b>

#### 2.4.2. Modified Rational Method

The rational method formula is an empirical relation that estimates the peak runoff discharge associated with a specific storm, and it is defined as follows:

$$Q_p = m C i A, \quad (2)$$

where  $Q_p$  is the peak discharge,  $m$  is the unit adjustment coefficient,  $C$  is the runoff coefficient,  $i$  is the rainfall intensity, and  $A$  is the area [25]. The runoff coefficient shows how much of the rainfall is converted to surface runoff and is defined as the ratio of the runoff depth to the precipitation depth, varying from zero to one [45]. In urban areas, the majority of rainfall is converted to runoff due to the prevalence of impervious surfaces, suggesting a  $C$  value typically closer to one.

In this research, one-meter land-cover data of Philadelphia were used to reclassify the surface of each subbasin into two categories: pervious and impervious. Then, two runoff coefficients of 0.95 and 0.35 were assigned for impervious and pervious areas, respectively, as required by the Philadelphia Water Department [44] for a conservative inlet design. These coefficients concur with the values used in previous studies [46–48]. To account for the effective impervious areas [2] in the city for runoff coefficient estimation, it was assumed that all the buildings footprints were not hydraulically connected to the surface runoff, and, therefore, they were excluded from calculations. Eventually, the peak runoff discharge was estimated by the following equation:

$$Q_p = \left[ (0.95 \times A_{imp}) + (0.35 \times A_{per}) \right] \times i, \quad (3)$$

where  $A_{imp}$  and  $A_{per}$  are impervious and pervious areas in each subbasin. In order to convert the peak discharge into the volume of the runoff, a trapezoidal hydrograph with constant peak discharge for the event duration was constructed. The time of concentration for inlets was considered five minutes [44] and, therefore, less than the duration of the event. The volume of the runoff was estimated by the following equation:

$$V = Q_p D, \quad (4)$$

where  $V$  is the volume of the runoff, and  $D$  is the duration of the storm [25]. GSIs slow water flow and act as a buffer between impervious areas and urban grey infrastructure [49]. Hence, they can play a crucial role in mitigating increased surface runoff [50]. The GSI watersheds in Philadelphia account for 0.7% of the total delineated area in the city. In this research, the rational method is used to show the effects of GSIs on peak runoff discharge reduction by defining two scenarios of considering GSIs as (1) pervious and (2) impervious. The difference between these scenarios quantifies and shows the effects of GSIs on peak runoff reduction.

### 2.4.3. NRCS Method

The NRCS method is a well-known and verified approach to predict runoff depth [14,24,51]. The runoff depth in this method is based on the rainfall, soil type, land use, and land cover characteristics, which are encapsulated in NRCS curve numbers (CN). The curve number for a watershed inherits the effects of soil type, vegetation cover, impervious areas, interception, and surface storage on runoff [3]. A higher curve number for a watershed indicates a greater likelihood that a watershed will generate more runoff.

In this research, a one-meter resolution curve number raster file was used to estimate the average curve number for each subbasin as follows:

$$CN_{Avg} = \sum CN_i \times A_i / A, \quad (5)$$

where  $CN_i$  and  $A_i$  are the curve numbers and area, respectively, in each subbasin [3]. The CN raster file was derived from the USDA's TR-55 (1986) [3] based on soil type, land use, and land cover. The CN of a few specific features in the urban landscape (i.e., community gardens and GSI installations) were derived from the published literature [35,36]. The curve numbers were assumed to remain constant through the event. Once the average CN was estimated for each subbasin, the maximum water retention in each subbasin could be estimated as follows:

$$S = \frac{1000}{CN_{Avg}} - 10, \quad (6)$$

where  $S$  is the maximum water retention in a subbasin, in inches. The runoff depth for the event was estimated by Equation (7):

$$Q = \frac{(P - I_a)^2}{(P - I_a) + S}, \quad (7)$$

where  $Q$  and  $P$  are the runoff and precipitation depths in inches, respectively, and  $I_a$  is the initial abstraction. By assuming initial abstraction on each subbasin is equal to  $0.2 S$  [3], the runoff depth can be estimated as follows:

$$Q = \frac{(P - 0.2 S)^2}{(P + 0.8 S)}. \quad (8)$$

## 2.5. Runoff Analysis Map

In this research, two different models—the modified rational and NRCS methods—were used to estimate surface runoff depths within delineated subbasins (the waterflow between subbasins was not considered). Since both models are widely used and verified, an integrative approach was used to combine both model results, to show different aspects of estimated runoff depths. To do this, three indices of 'Agreement', 'Maximum', and 'Average' were defined.

### 2.5.1. Agreement Index

The agreement index intends to show the probability of the surface runoff exceeding a given threshold ( $Thr$ ) predicted by the two models. The conditions used for defining the agreement index are shown in Table 4.

**Table 4.** The agreement index indicates the agreement between the modified rational and NRCS models. The  $H_{RH}$  and  $H_{NRCS}$  are the runoff depths estimated by the rational and NRCS methods, respectively, and  $Thr$  is the threshold depth equal to 5 centimeters.

Condition	Agreement (%)
$(H_{RH} > Thr) \text{ AND } (H_{NRCS} > Thr)$	100
$(H_{RH}) \text{ OR } (H_{NRCS}) < Thr$	50
$(H_{RH} < Thr) \text{ AND } (H_{NRCS} < Thr)$	0

A higher agreement between two models indicates greater confidence that surface runoff will exceed the threshold. The threshold for surface runoff in this research was set to 5 centimeters, indicating the initiation of flood conditions, supported by other literature [52].

### 2.5.2. Maximum Index

To show the highest possible runoff depth and the worst-case scenario for each subbasin, the maximum factor was defined as the maximum water depth between two models:

$$Maximum = Maximum(H_{RH}, H_{NRCS}) \quad (9)$$

The maximum factor is an important index for situations where the consequences of excessive runoff are dire. For instance, the maximum index can be used to find areas in the city that are dangerous for driving through during the storm, due to high inundation levels.

### 2.5.3. Average Index

The average index combines the results of both models and was defined as the average runoff depth predicted by both models:

$$Average = 0.5 \times (H_{RH} + H_{NRCS}) \quad (10)$$

Areas with higher average index indicate that both models, on average, predict high levels of surface runoff.

## 3. Results

In total, 80,453 subbasins were identified in Philadelphia, with mean and median areas of 2935 and 204 square meters, respectively. More than 76 percent of the subbasins fall below the average area, while about 50 percent of the subbasins are below the median. This implies that the area of subbasins is positively skewed, with a large number of small subbasins.

### 3.1. Modified Rational vs NRCS Runoff Depths

The runoff depths for different durations of the design storm (Table 3) were estimated by both the modified rational and NRCS methods and presented in Figure 2.

The NRCS model incorporates land-cover data to assess initial abstraction and runoff depth consequently. The modified rational model, however, is based on the percentage of impervious area. The comparison between runoff depths for different storm durations, varying from five minutes to 24 h, obtained from both models showed that, for lower storms, the runoff depths estimated by the NRCS method are lower than the ones estimated by the rational method (Figure 3A,B). However, as the duration of the storm increases, the surface runoff depths estimated by both models converge. As a result, both models performed relatively similar for the 24-h design storm. Therefore, the 24-h storm was selected for further analysis in this research. The points in Figure 3 are partially transparent so that higher point densities are shown in darker colors. The outlier points result from clipping



buildings out of the watershed feature class and from extremely flat areas in the DEM surface due to terrain smoothing.

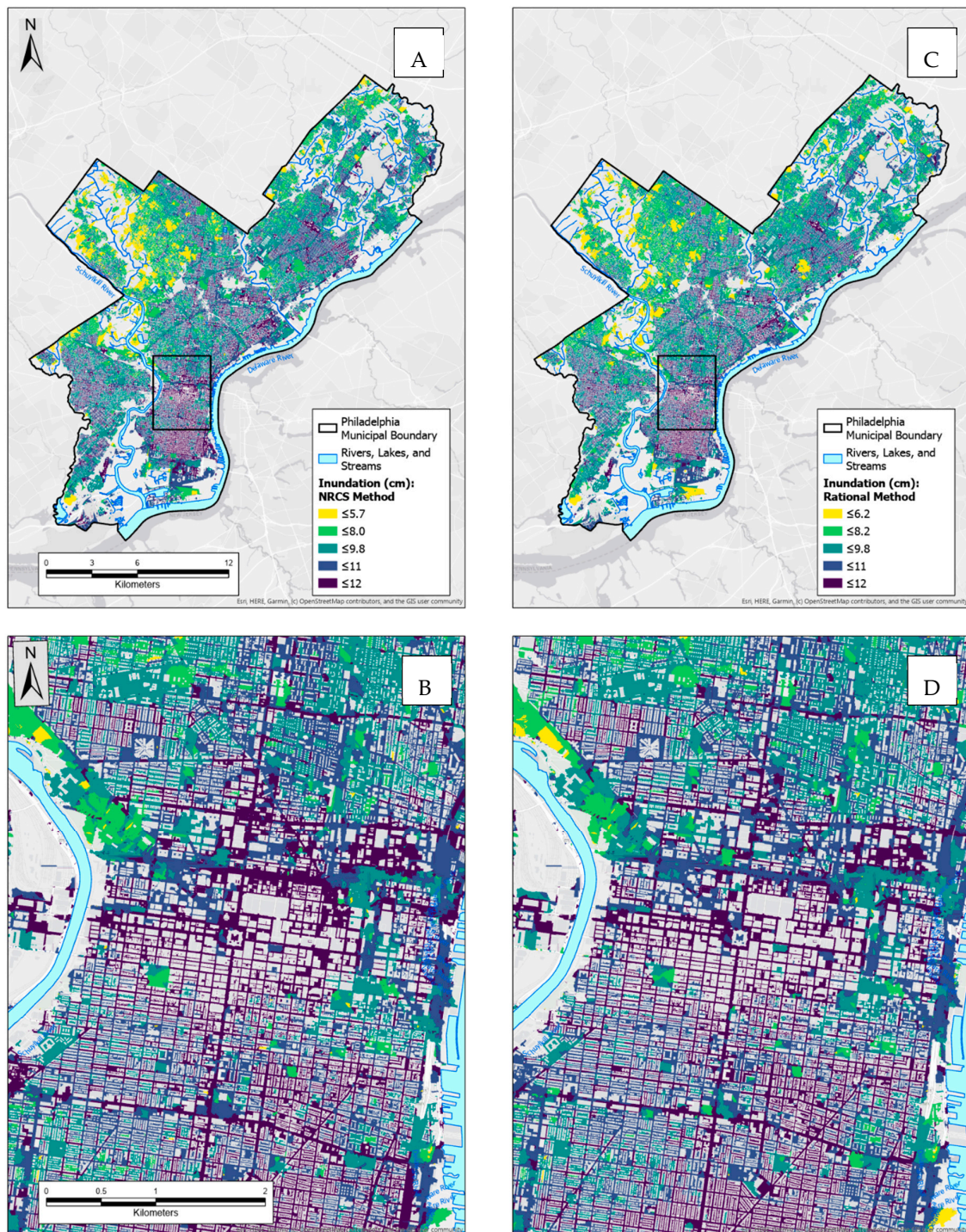


**Figure 2.** Comparison of estimated runoff depths predicted by the NRCS (A,B) and rational method (C,D) for city of Philadelphia and Center City for 24-h, 10-year storm.



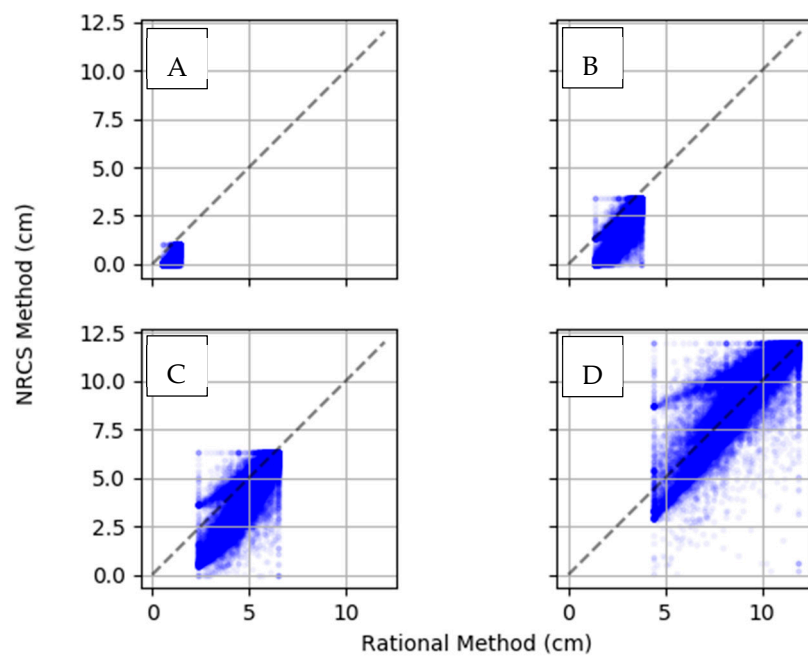


**Figure 3.** Change in runoff depth estimated by the modified rational and NRCS models for the 10-year design storm for the duration of (A) 5 min, (B) 30 min, (C) 3 h, and (D) 24-h.

The difference in runoff depths between two models was estimated for all subbasins by subtracting the runoff depth of the NRCS model from the runoff depth obtained by the modified rational method. The results showed that the difference between estimated runoff depths of the two models is less than 0.88 cm for the majority of subbasins (Figure 4).

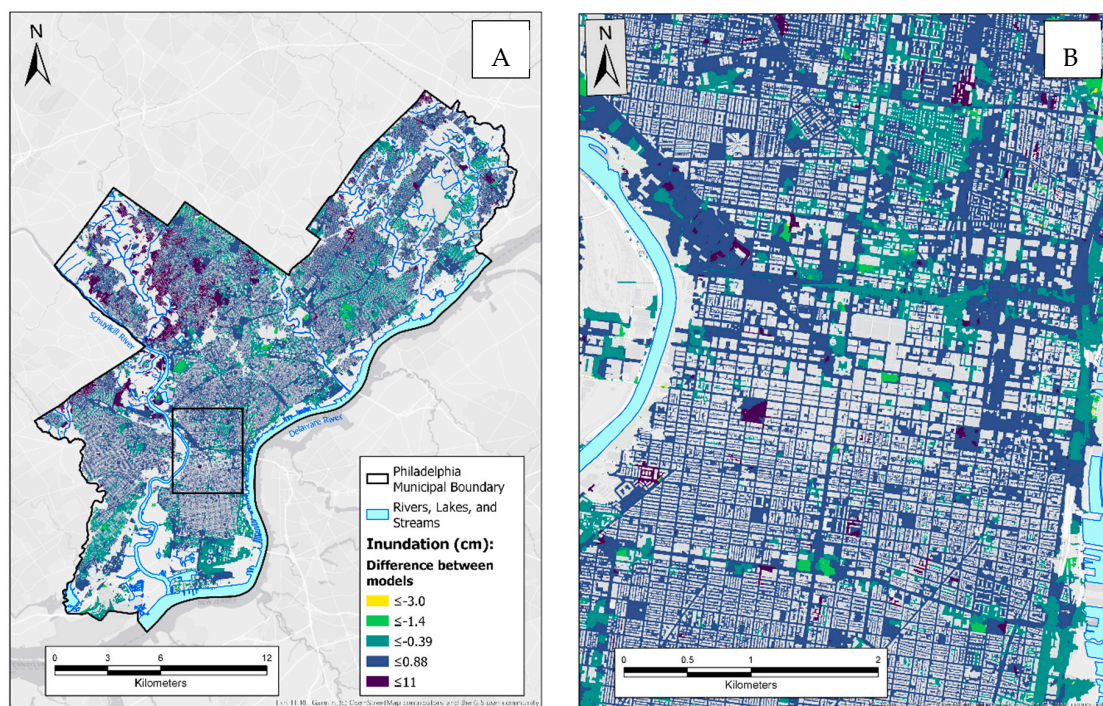


**Figure 4.** The difference in runoff depth between runoff depths estimated by the modified rational and NRCS methods for all subbasins in (A) city of Philadelphia and (B) Center City.

### 3.2. Effects of GSIs on Runoff Reduction

GSIs in Philadelphia account for 0.7% of all delineated watershed area. Runoff estimation showed that 0.65% to 0.70% of runoff from a 24-h, 10-year storm in Philadelphia can be mitigated by current GSIs. To show the effects of GSIs on the reduction of peak runoff discharge, the rational method was used to estimate the peak discharge for two scenarios. In the first scenario, the GSIs throughout the city were assumed to be entirely impervious with a runoff coefficient of 0.95. Then, the peak discharges for subbasins were estimated. In the second scenario, all GSIs were assumed completely pervious with the runoff coefficient of 0.35, and peak discharges were estimated. The difference in the peak discharge values of each scenario showed the effects of GSIs on attenuating the peak runoff discharge. The results showed that GSIs are capable of reducing the peak runoff discharge from 0.01% to 63.2%, depending upon the ratio of the area of the GSI to the area of subbasin (Figure 5). This is in line with the findings of Lord [53], and Traver and Ebrahimian [54].

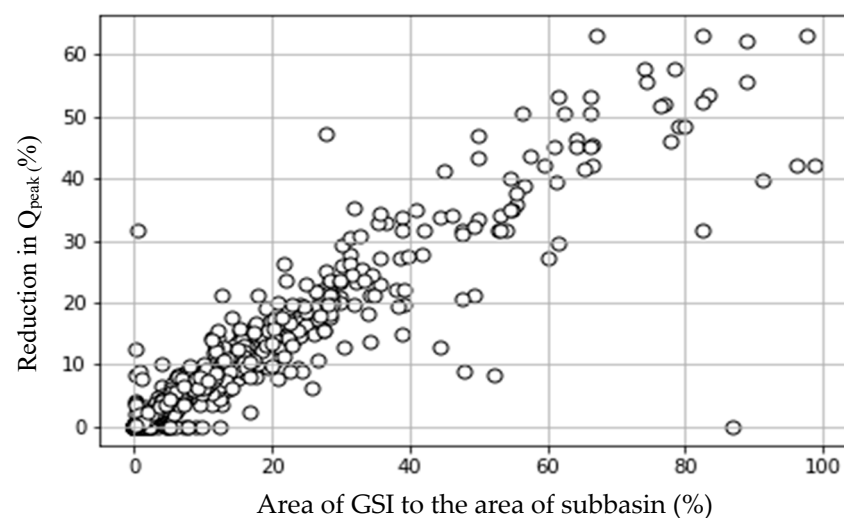


**Figure 5.** The relation between area of GSI and reduction in peak runoff discharge.

### 3.3. Runoff Analysis Map

#### 3.3.1. Agreement Index Map

The agreement between models to predict the surface runoff depth of a 10-year, 24-h storm exceeding five centimeters was estimated for the City of Philadelphia and mapped in Figure 6. The results showed that for a 24-h storm, the majority of the subbasins experienced runoff depths more than the threshold depth (Section 2.5.1).

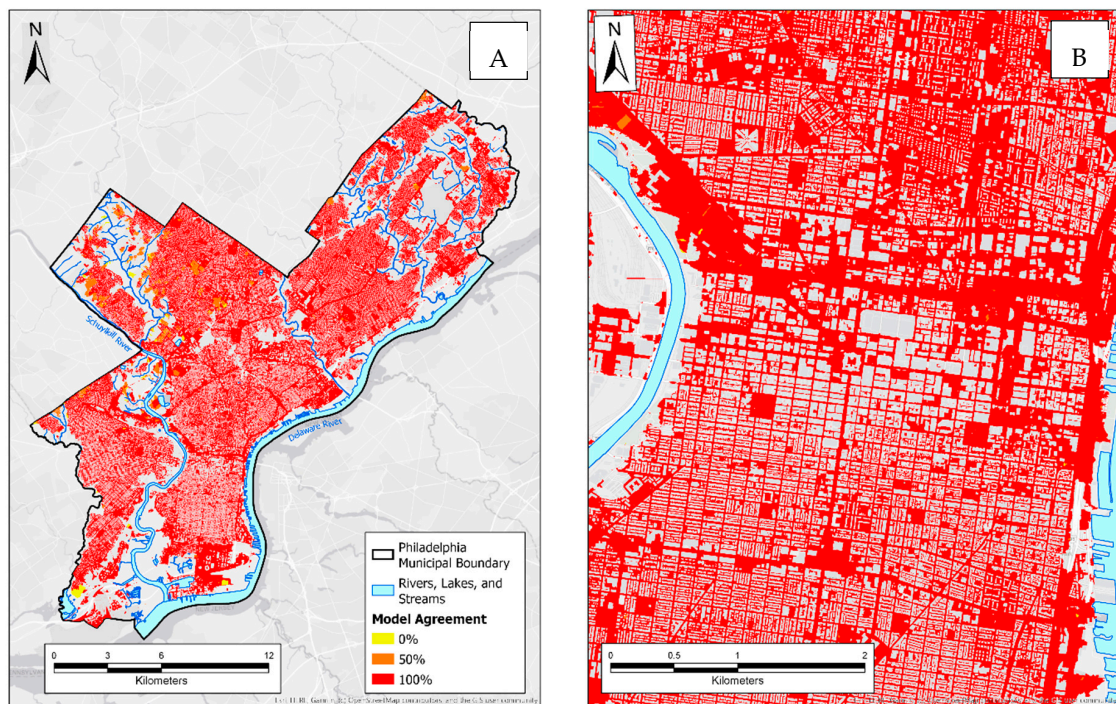


**Figure 6.** The Agreement index map of the surface runoff depth resulted from the 10-year, 24-h storm is depicted for city of Philadelphia (A) and Center City (B). Red areas show where both the modified rational and NRCS methods agree on surface runoff depth exceeding the threshold of 5 cm.

### 3.3.2. Maximum Index Map

The maximum index map aims to display the highest runoff depth (worst-case scenario), resulting from the 10-year, 24-h storm. Figure 7 shows the maximum possible runoff depths estimated by the modified rational or NRCS methods for Philadelphia (Section 2.5.2). The results showed that, for the 24-h, 10-year storm in Philadelphia, GSIs can collect 0.3% of the maximum predicted runoff depths.



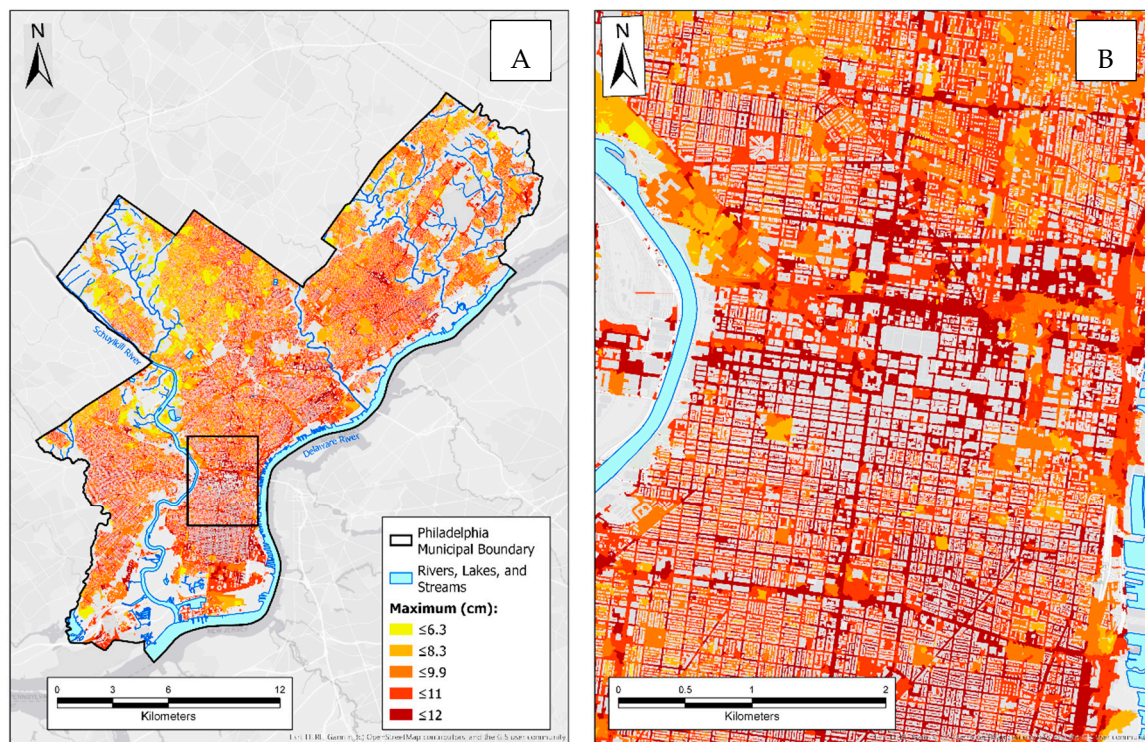


**Figure 7.** Maximum estimated runoff depths for each subbasin, estimated by the NRCS or rational models for a 24-h, 10-year storm for city of Philadelphia (A) and Center City (B).

### 3.3.3. Average Index Map

The average index map aims to incorporate the runoff depth results from both the modified rational and NRCS models, to represent an integral form of inundation (Figure 8). The average index parameter is the average runoff depths obtained from both models. In that way, in areas where the average index is higher, there is more confidence that both models predict higher runoff in such areas on average (Section 2.5.3). The results showed that subbasins with GSIs are capable of reducing the average index for the whole city (average inundation) up to 1.2%.

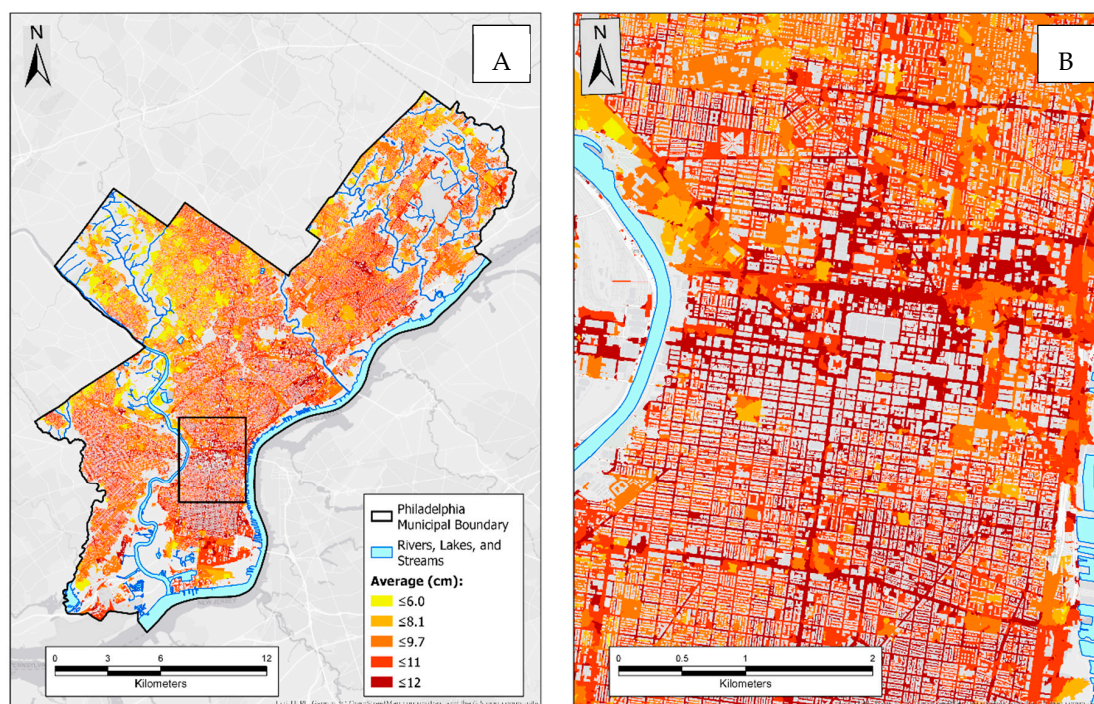


**Figure 8.** The average index map shows the average runoff depth estimated by the NRCS and modified rational models for 24-h, 10-year storm for city of Philadelphia (A) and Center City (B).

#### 4. Discussion

The results of the models agree that extensive parts of the city are prone to flooding. This, overall, is in agreement with the extent and level of damage throughout the city reported following flash flooding caused by 127 mm of rainfall (relatively close to rain depth used in this study, equal to 125.7 mm,) on June, 2019 in Philadelphia [38,55]. However, the exact extent of the flooding and inundation of this event is not available to compare with the results of this study.

Efficient, well-designed GSIs are capable of reducing the volume and the peak of runoff up to 85%–100% [56]. However, depending upon the GSI type and its characteristics, the volume of runoff reduction can vary from 2% to 45% [57,58]. Many municipalities in the Mid-Atlantic region, including Philadelphia, have set a goal to reduce runoff by 10%–20%, using GSIs [59]. The results from this research showed that GSI watersheds in Philadelphia account for 0.71% of the total delineated watershed area and can reduce the peak runoff discharge in subbasins from 0.01% to 63.2%, depending upon the size of the GSI relative to the area of the subbasin in which it is located. However, for the whole city, 0.65%–0.7% of the peak discharge can be reduced by GSIs on average. This helps municipalities to quantify the required area of GSI needed to achieve desired runoff reductions.

The estimated runoff depths for the city of Philadelphia subbasins obtained by the modified rational method were less divergent than those obtained by the NRCS methods in larger storms. In contrast, the average difference between two models in small storms was greater (Figure 9). More specifically, the NRCS method tended to underestimate the surface runoff depth in small storms relative to the modified rational method. That shows that the NRCS method was more sensitive in small storms, in agreement with the findings of Grove et al. [23] and Hawkins [60]. Small storms have higher intensity (Table 3) which impacted peak runoff and runoff depth in the modified rational method (Equations (2) and (4)). Conversely, the rainfall intensity in larger storms decreases while the precipitation increases. This caused the runoff depths estimated by the NRCS method to increase.



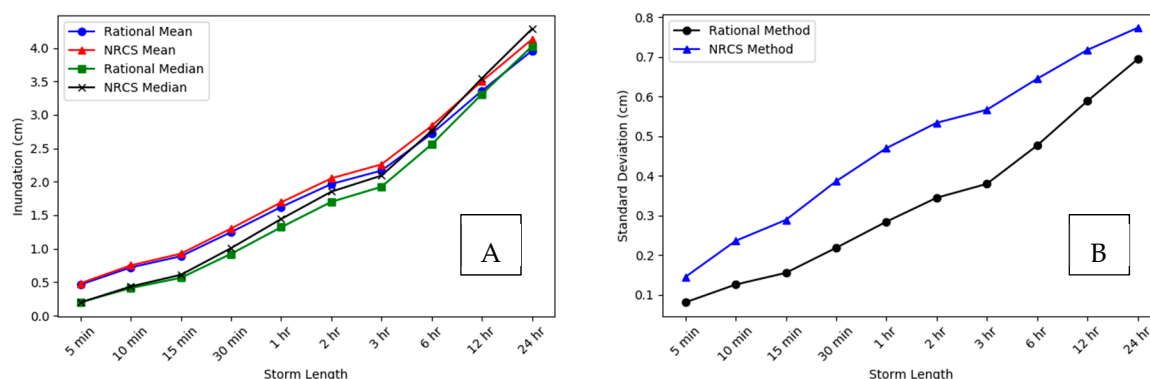


**Figure 9.** The mean and median runoff depths (A) and standard deviation (B) of all subbasins in Philadelphia, estimated by the NRCS and rational models for a 24-h, 10-year storm.

Initial abstraction in the NRCS method represents all losses before the runoff initiates, and this includes evapotranspiration, surface depression, and infiltration [3].

In this research, the initial abstraction was assumed to be  $0.2 S$  ( $I_a$  in Equation (7)), as suggested by the NRCS runoff estimation manual [3]. However, a value of  $0.05 S$  for  $I_a$  in urban watersheds is also suggested in some literature, and this implies a higher rate of runoff [36,51]. For this research, runoff depths for both initial abstractions were estimated. The results showed that, by decreasing  $I_a$  to  $0.05 S$ , the maximum runoff depths in watersheds increased slightly. However, changes in mean runoff depth and the resulting runoff analysis maps were negligible. On the other side, the storm duration for this research was set to 24-h, based on the NRCS runoff manual suggestion [3]. These analyses showed that, for 24-h storm, change in initial abstraction caused a minimal difference between runoff depths estimated by the NRCS and modified rational methods.

Histograms of estimated runoff depths for the 10-year, 24-h storm obtained by both models (Figure 10) showed that the highest runoff depths were approximately five times more frequent than smaller runoff depths in Philadelphia. This implies that there is a substantial number of large subbasins within Philadelphia that potentially are flooded simultaneously. The standard deviation of the runoff depths from the NRCS method was slightly higher than that of the modified rational method, implying greater variability in runoff depths estimated by the NRCS method. This is likely due to variations in curve numbers throughout the watershed.

In the absence of measured runoff-depth data for model verification, the sensitivity of the models relative to the CN and precipitation depth values was analyzed (Figure 11). The runoff depth obtained from the NRCS method is a monotonic, nonlinear function of CN. Figure 11 shows the sensitivity of the NRCS model with respect to precipitation and CN. On the other hand, the runoff depth obtained from the modified rational method is linearly correlated to  $C$ , the area of the watershed and the precipitation intensity. That implies that any percent of change in  $C$ , area, or precipitation intensity results in the same percent of change in runoff depth.

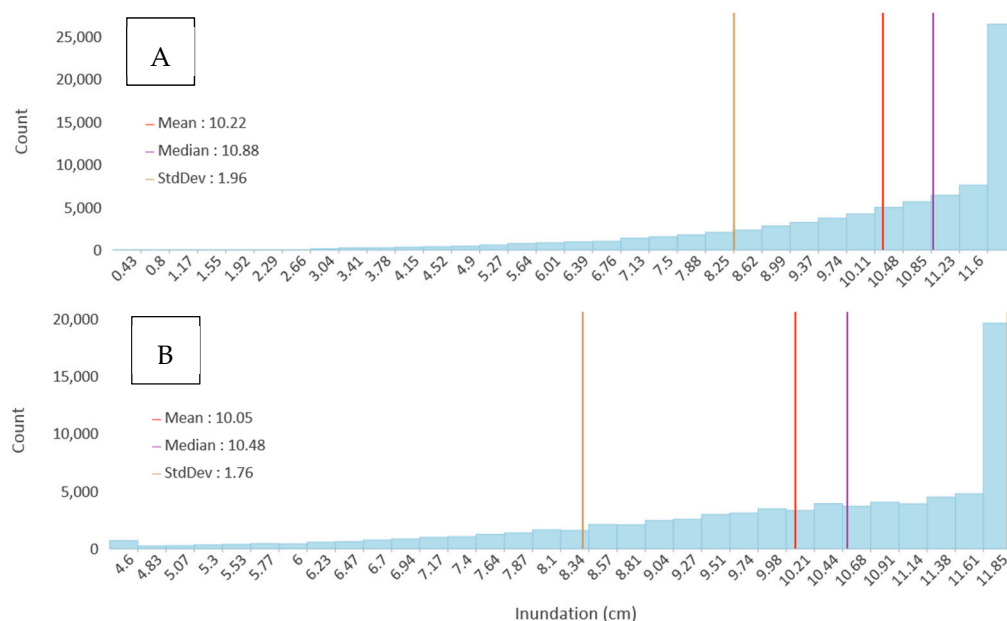


**Figure 10.** The frequency of runoff depths for all subbasins in Philadelphia, estimated by the (A) NRCS and (B) modified rational models for 24-h, 10-year storm.

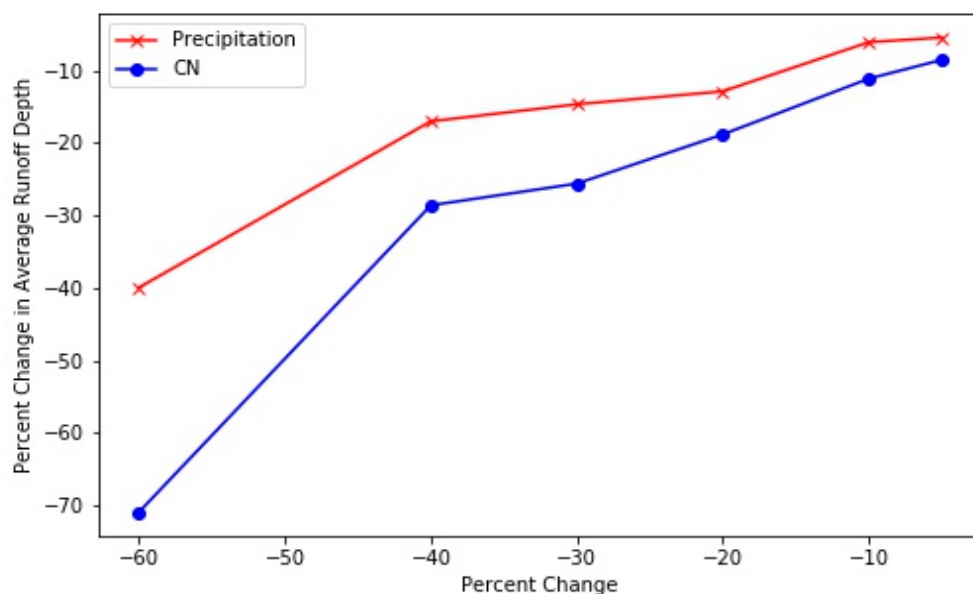


**Figure 11.** Sensitivity of the developed NRCS model relative to CN and precipitation.

## 5. Model Limitations

Limitations of this study include elements in subbasin delineation methodology and runoff estimation, such as substantially flat areas, relatively large subbasins, or the presence of large water bodies in a watershed. In addition, a lack of measured runoff-depth data is a great challenge for model verification. The rational method is limited to watersheds less than 200 acres in area. Therefore, any subbasins exceeding this threshold were not included in this analysis. Additionally, subbasins that intersected bodies of water, particularly rivers and streams, tended to be excessively large and did not appear to accurately represent drainage characteristics in these areas. These subbasins were also excluded from this analysis. The total area of removed subbasins was estimated to be 43 square kilometers (eleven percent of the study area), including rivers, creeks, and extremely large subbasins.

Subbasins in extremely flat areas often appeared unnatural, forming extremely small or very long and narrow shapes. These subbasins remained in the analysis, but this issue should be further investigated in future research. In addition, there were some GSI shape files in the data (polygons) that were not connected to any inlet which needs further investigation. Finally, the current model needs further adjustment to account for the interconnection of the water flow between subbasins.

## 6. Conclusions

In this research, we developed an automated framework which uses high-resolution topographic data to delineate micro-subbasins in citywide-scale watersheds. The model was applied to Philadelphia, PA, a fully urbanized watershed. The modified rational and NRCS models were used to estimate surface runoff depth for each micro-subbasin. The comparison between model results showed that, for a 24-h, 10-year storm, both models performed fairly similarly. The effect of green stormwater infrastructure (GSI) on peak runoff reduction was tested by using the rational method and in two separate scenarios. In the first scenario, GSI in subbasins were assumed to be fully impervious. In the second scenario, the GSI was treated as fully pervious.

The differences in peak discharge for these two scenarios quantified the effects of GSI on peak runoff reduction. The results showed that 13 km<sup>2</sup> (0.71%) of the Philadelphia area drains into the GSIs, resulting in peak runoff mitigation that varies from 0.01% to 63.2% in GSI subbasins. However, only less than 1% of the peak runoff discharge can be reduced by GSIs for the whole city on average.

To identify areas prone to excessive runoff and flooding, a framework was defined to generate runoff analysis maps depicting model agreement, maximum runoff depth, and average runoff depth for the study area. The agreement map shows the agreement between the rational and NRCS models in predicting runoff depth exceeding a predetermined threshold value. The results showed that both models predicted that the majority of Philadelphia will experience at least 5 cm of runoff during a 24-h, 10-year storm. The maximum map was intended to show the maximum runoff depth for each subbasin and can be used to identify locations where particularly damaging levels of inundation could occur. Finally, the average index was defined as the mean runoff depth estimated by both models. The average map identified critical areas throughout the city, with a particularly high concentration occurring in Center City, Philadelphia. Runoff analysis maps provide critical information that can be coupled with demographic data to identify particularly vulnerable areas in the City of Philadelphia.

This work also creates an opportunity for deepening the science and engineering community's knowledge of urban stormwater dynamics and can be used toward the applications of the surface-runoff modeling in urban management. The integrated methodology and type of data used in this study create a framework for analyzing stormwater systems on a city-scale. Moreover, the output of the current framework, including delineated micro-subbasins, can be complimentary to existing stormwater management methods, through integration with a wide range of spatial hydrologic and hydraulic models. Future work can incorporate an assessment of the impact of GSI in terms of agreement, maximum, or average maps, to investigate the relationship between surface runoff in small-scale watersheds, and demographic and socioeconomic characteristics, as well as other environmental phenomena, such as surface temperature on ecosystem services in the City of Philadelphia.

**Author Contributions:** Conceptualization, H.H., M.C., P.K., and V.B.S.; methodology, H.H. and M.C.; software, M.C. and H.H.; validation, H.H., M.C., P.K., and V.B.S.; formal analysis, H.H. and M.C.; resources, P.K. and V.B.S.; writing—original draft preparation, H.H. and M.C.; writing—review and editing, H.H., M.C., P.K., and V.B.S.; visualization, M.C.; supervision, P.K. and V.B.S.; project administration, P.K. and V.B.S.; funding acquisition, P.K. and V.B.S. All authors have read and agreed to the published version of the manuscript.

**Funding:** This research received no external funding and was funded by Villanova College of Engineering.

**Acknowledgments:** The authors would like to thank Nicole Marks, Victoria Bill, Kirsten Ahn, and Ward Barnes for sharing their insight with us during the creation of this manuscript.

**Conflicts of Interest:** The authors declare no conflicts of interest. The funders had no role in the design of the study; in the collection, analyses, or interpretation of data; in the writing of the manuscript; or in the decision to publish the results.

## References

1. Second, M.L.; Wheeler, H.S.; Onof, C. The significance of spatial rainfall representation for flood runoff estimation: A numerical evaluation based on the Lee catchment, UK. *J. Hydrol.* **2007**, *347*, 116–131. [\[CrossRef\]](#)
2. Alley, W.M.; Veenhuis, J.E. Effective Impervious Area in Urban Runoff Modeling. *J. Hydraul. Eng.* **1983**, *109*, 313–319. [\[CrossRef\]](#)
3. USDA TR-55. Urban Hydrology for Small Watersheds. Available online: <http://www.ncbi.nlm.nih.gov/pmc/pub/filespec-images/> (accessed on 28 September 2019).
4. Corbett, C.W.; Wahl, M.; Porter, D.E.; Edwards, D.; Moise, C. Nonpoint source runoff modeling. A comparison of a forested watershed and an urban watershed on the South Carolina coast. *J. Exp. Mar. Bio. Ecol.* **1997**, *213*, 133–149. [\[CrossRef\]](#)
5. United Nations News. Available online: <https://www.un.org/development/desa/en/news/population/2018-revision-of-world-urbanization-prospects.html> (accessed on 28 September 2019).
6. Wu, J.S.; Allan, C.J.; Saunders, W.L.; Evett, J.B. Characterization and Pollutant Loading Estimation for Highway Runoff. *J. Environ. Eng.* **1998**, *124*, 584–592. [\[CrossRef\]](#)
7. Hammond, M.J.; Chen, A.S.; Djordjević, S.; Butler, D.; Mark, O. Urban Flood Impact Assessment: A State-of-the-Art Review. *Urban Water J.* **2015**, *12*, 14–29. [\[CrossRef\]](#)
8. Banasik, K.; Hejduk, A. Ratio of Basin Lag Times for Runoff and Sediment Yield Processes Recorded in Various Environments. In Proceedings of the International Association of Hydrological Sciences, New Orleans, LA, USA, 11–14 December 2014; pp. 163–169.
9. Genereux, D.P. Comparison of Methods for Estimation of 50-Year Peak Discharge from a Small, Rural Watershed in North Carolina. *Environ. Geol.* **2003**, *44*, 53–58. [\[CrossRef\]](#)
10. Choi, K.S.; Ball, J.E. Parameter Estimation for Urban Runoff Modelling. *Urban Water* **2002**, *4*, 31–41. [\[CrossRef\]](#)
11. Bisht, D.S.; Chatterjee, C.; Kalakoti, S.; Upadhyay, P.; Sahoo, M.; Panda, A. Modeling Urban Floods and Drainage Using SWMM and MIKE URBAN: A Case Study. *Nat. Hazards* **2016**, *84*, 749–776. [\[CrossRef\]](#)
12. Hosseiny, H.; Smith, V. Two Dimensional Model for Backwater Geomorphology: Darby Creek, PA. *Water* **2019**, *11*, 2204. [\[CrossRef\]](#)
13. Brezonik, P.L.; Stadelmann, T.H. Analysis and predictive models of stormwater runoff volumes, loads, and pollutant concentrations from watersheds in the twin cities metropolitan area, Minnesota, USA. *Water Res.* **2002**, *36*, 1743–1757. [\[CrossRef\]](#)
14. Sathish Kumar, D.; Arya, D.S.; Vojinovic, Z. Modeling of urban growth dynamics and its impact on surface runoff characteristics. *Comput. Environ. Urban* **2013**, *41*, 124–135. [\[CrossRef\]](#)
15. Shamsi, U.M. Arc Hydro: A Framework for Integrating GIS and Hydrology. *J. Water Manag. Model.* **2008**, *6062*, 165–182. [\[CrossRef\]](#)
16. Ji, S.; Qiuwen, Z. A GIS-Based Subcatchments Division Approach for SWMM. *Open Civ. Eng. J.* **2015**, *9*, 515–521. [\[CrossRef\]](#)
17. Parece, T.E.; Campbell, J.B. Delineating Drainage Networks in Urban Areas. In Proceedings of the ASPRS 2014 Annual Conference, Louisville, Kentucky, 23–27 March 2014; pp. 7–10.
18. Hans, Z.; Hallmark, S.; Souleyrette, R.; Tenges, R.; Veneziano, D. *Use of LiDAR-Based Elevation Data for Highway Drainage Analysis: A Qualitative Assessment*; MTC Project 2001-02, CTRE Project 01-98; Midwest Transportation Consortium c/o Iowa State University: Ames, IA, USA, 2003 October.
19. Vaughn, C. Determining an Optimal DEM Resolution and Evaluating Low Impact Redevelopment through Field Monitoring and LiDAR. Master's Thesis, Villanova University, Villanova, PA, USA, May 2018.
20. Chiew, F.H.S.; McMahon, T.A. Modelling runoff and diffuse pollution loads in urban areas. *Water Sci. Technol.* **1999**, *39*, 241–248. [\[CrossRef\]](#)
21. Arnell, V. Estimating Runoff Volumes from Urban Areas. *Water Resour. Bull.* **1982**, *18*, 383–387. [\[CrossRef\]](#)
22. Kuichling, E.; Hering, R. *The Relation between the Rainfall and the Discharge of Sewers in Populous Districts*; American Society of Civil Engineers: New York, NY, USA, 1889.
23. Grove, M.; Harbor, J.; Engel, B. Composite vs. Distributed Curve Numbers: Effects on Estimates of Storm Runoff Depths. *J. Am. Water Resour. Assoc.* **1998**, *34*, 1015–1023. [\[CrossRef\]](#)
24. Banasik, K.; Krajewski, A.; Sikorska, A.; Hejduk, L. Curve Number Estimation for a Small Urban Catchment from Recorded Rainfall-Runoff Events. *Arch. Environ. Prot.* **2014**, *40*, 75–86. [\[CrossRef\]](#)

25. Dhakal, N.; Fang, X.; Thompson, D.B.; Cleveland, T.G. Modified Rational Unit Hydrograph Method and Applications. *Water Manag.* **2014**, *167*, 381–393. [CrossRef]
26. Poertner, H.G. *Practices in Detention of Urban Stormwater Runoff: An Investigation of Concepts, Techniques, Applications, Costs, Problems, Legislation, Legal Aspects, and Opinions*; American Public Works Association: Chicago, IL, USA, 1974.
27. Sweet, W.V.; Dusek, G.; Marcy, D.; Carbin, G.; Marra, J.J. *2018 State of U.S. High Tide Flooding with a 2019 Outlook*; NOAA Technical Report NOS CO-OPS: Silver Spring, MD, USA, 2019 June.
28. *ArcGIS Pro*; Environmental Systems Research Institute: Redlands, CA, USA, 2018.
29. Maidment, D. *Arc Hydro: GIS for Water Resources*; ESRI Press: Redlands, CA, USA, 2002.
30. An Automated Method for Delineating Drainage Areas of Green Stormwater Infrastructure Using GIS. Available online: [https://www.esri.com/en-us/industries/water/segments/water-utilities/green-stormwater-case-study?adumkts=industry\\_solutions&aduse=water&aduin=wws&aduc=email&adum=drip&utm\\_Source=email&aduca=wws\\_community&aduco=newsletter-W19-ACEpipe&adut=385748-Esri-News-](https://www.esri.com/en-us/industries/water/segments/water-utilities/green-stormwater-case-study?adumkts=industry_solutions&aduse=water&aduin=wws&aduc=email&adum=drip&utm_Source=email&aduca=wws_community&aduco=newsletter-W19-ACEpipe&adut=385748-Esri-News-) (accessed on 5 October 2019).
31. Jahangiri, H.M. An Automated Method for Delineating Drainage Areas of Green Stormwater Infrastructures Using GIS. Master's Thesis, Villanova University, Pennsylvania, USA, December 2018.
32. Mays, L.W. *Water Resources Engineering*, 2nd ed.; John Wiley & Sons: Scottsdale, AZ, USA, 2010.
33. Chow, V.T.; Maidment, D.; Mays, L.W. *Applied Hydrology*; Clark, B.J., Morriss, J., Eds.; McGraw-Hill Book Co.: New York, NY, USA, 1988.
34. American Fact Finder. Available online: <https://factfinder.census.gov/faces/tableservices/jsf/pages/productview.xhtml?src=bkmk> (accessed on 5 October 2019).
35. Shade, C.; Kremer, P. Predicting Land Use Changes in Philadelphia Following Green Infrastructure Policies. *Land* **2019**, *8*, 28. [CrossRef]
36. Shade, C. Green Infrastructure Policy as a Strategy for Climate Change Adaptation in Philadelphia. Master's Thesis, Villanova University, Villanova, PA, USA, May 2019.
37. NOAA. National Weather Service Forecast Office. Available online: <https://w2.weather.gov/climate/index.php?wfo=phi> (accessed on 9 June 2019).
38. Murrell, D. It Seems NOAA Wasn't Kidding About Those Philly Flood Predictions. Available online: <https://www.phillymag.com/news/2019/07/12/philadelphia-flood-future-noaa/> (accessed on 28 September 2019).
39. Hanna, J.; Sutton, J. CNN News. Available online: <https://www.cnn.com/2019/06/20/us/philadelphia-area-flooding-new-jersey-rescues-wxc/index.html> (accessed on 9 June 2019).
40. OpenDataPhilly. Shapefiles of Philadelphia. Available online: <https://www.opendataphilly.org/dataset> (accessed on 10 June 2019).
41. Pennsylvania Spatial Data Access. PAMAP Program - 3.2 ft Digital Elevation Model. Available online: <https://www.pasda.psu.edu/uci/DataSummary.aspx?dataset=1247> (accessed on 10 June 2019).
42. Pennsylvania Spatial Data Access | Data Summary. Available online: <http://www.pasda.psu.edu/uci/DataSummary.aspx?dataset=1048> (accessed on 12 October 2018).
43. Open Data Philly. Available online: <https://www.opendataphilly.org/> (accessed on 6 January 2019).
44. PWD Stormwater Plan Review. Philadelphia Water Department. Available online: <https://www.pwdplanreview.org/manual/chapter-3/3.4-how-to-show-compliance> (accessed on 15 July 2019).
45. Şen, Z.; Altunkaynak, A. A Comparative Fuzzy Logic Approach to Runoff Coefficient and Runoff Estimation. *Hydrol. Process.* **2006**, *20*, 1993–2009. [CrossRef]
46. Bedient, P.B.; Huber, W.C.; Vieux, B.E. *Hydrology and Floodplain Analysis*, 4th ed.; Prentice Hall: Upper Saddle River, NJ, USA, 2008.
47. Sriwongsitanon, N.; Taesombat, W. Effects of Land Cover on Runoff Coefficient. *J. Hydrol.* **2011**, *410*, 226–238. [CrossRef]
48. Thanapura, P.; Helder, D.L.; Burckhard, S.; Warmath, E.; O'Neill, M.; Galster, D. Mapping Urban Land Cover Using QuickBird NDVI Image and GIS Spatial Modeling for Runoff Coefficient Determination. *Photogramm. Eng. Rem. Sens.* **2007**, *73*, 57–65. [CrossRef]
49. Ebrahimian, A.; Gulliver, J.S.; Wilson, B.N. Effective Impervious Area for Runoff in Urban Watersheds. *Hydrol. Process.* **2016**, *30*, 3717–3729. [CrossRef]



50. Maragno, D.; Gaglio, M.; Robbi, M.; Appiotti, F.; Fano, E.A.; Gissi, E. Fine-Scale Analysis of Urban Flooding Reduction from Green Infrastructure: An Ecosystem Services Approach for the Management of Water Flows. *Ecol. Modell.* **2018**, *386*, 1–10. [CrossRef]
51. Lim, K.J.; Engel, B.A.; Muthukrishnan, S.; Harbor, J. Effects of Initial Abstraction and Urbanization on Estimated Runoff Using CN Technology. *J. Am. Water Resour. Assoc.* **2006**, *42*, 629–643. [CrossRef]
52. Zarzar, C.M.; Hosseiny, H.; Siddique, R.; Gomez, M.; Smith, V.; Mejia, A.; Dyer, J. A Hydraulic MultiModel Ensemble Framework for Visualizing Flood Inundation Uncertainty. *JAWRA J. Am. Water Resour. Assoc.* **2018**, *54*, 807–819. [CrossRef]
53. Lord, L.E. Evaluation of Nitrogen Removal and Fate within A Bioinfiltration Stormwater Control Measure. Available online: <https://search.proquest.com/openview/74abe6142351e5a10723bd08687ea824/1.pdf?pq-origsite=gscholar&cbl=18750&diss=y> (accessed on 15 July 2019).
54. Traver, R.G.; Ebrahimian, A. Dynamic Design of Green Stormwater Infrastructure. *Front. Environ. Sci. Eng.* **2017**, *11*. [CrossRef]
55. NBC10 First Alert Weather Team. NBC10. Available online: <https://www.nbcphiladelphia.com/weather/First-Alert-Weather-Severe-Storms-Tropical-Downpours-Flooding-Lightning-Winds-Philadelphia-Pennsylvania-New-Jersey-Delaware-524438061.html> (accessed on 9 June 2019).
56. Liu, W.; Chen, W.; Peng, C. Assessing the effectiveness of green infrastructures on urban flooding reduction: a community scale study. *Ecol. Modell.* **2014**, *291*, 6–14. [CrossRef]
57. Xie, J.; Chen, H.; Liao, Z.; Gu, X.; Zhu, D.; Zhang, J. An integrated assessment of urban flooding mitigation strategies for robust decision making. *Environ. Model. Softw.* **2017**, *95*, 143–155. [CrossRef]
58. Lucas, W.C.; Sample, D.J. Reducing combined sewer overflows by using outlet controls for green stormwater infrastructure: case study in Richmond, Virginia. *J. Hydrol.* **2015**, *520*, 473–488. [CrossRef]
59. Pennino, M.J.; McDonald, R.I.; Jaffe, P.R. Watershed-scale impacts of stormwater green infrastructure on hydrology, nutrient fluxes, and combined sewer overflows in the mid-Atlantic region. *Sci. Total Environ.* **2016**, *565*, 1044–1053. [CrossRef] [PubMed]
60. Hawkins, R.H. The Importance of Accurate Curve Numbers in the Estimation of Storm Runoff. *Water Res. Bull.* **1975**, *11*, 11–890. [CrossRef]



© 2020 by the authors. Licensee MDPI, Basel, Switzerland. This article is an open access article distributed under the terms and conditions of the Creative Commons Attribution (CC BY) license (<http://creativecommons.org/licenses/by/4.0/>).